

# Oversampled Orthogonal Frequency Division Multiplexing in Doubly Selective Fading Channels

Jingxian Wu, *Member, IEEE*, and Yahong Rosa Zheng, *Senior Member, IEEE*

**Abstract**—A new oversampled orthogonal frequency division multiplexing (OOFDM) scheme is proposed for doubly selective fading environment. The proposed OOFDM scheme employs oversampling in the time domain and linear processing in the frequency domain, both at the receiver without changing the structure of conventional orthogonal frequency division multiplexing (OFDM) transmitters. The time-frequency processing enables a two dimensional Doppler-frequency grid of the fading channel, such that each data symbol is modeled equivalently as being transmitted at multiple subcarriers and various Doppler spreads simultaneously, while retaining the same spectral efficiency as conventional OFDM systems. Optimum combining ensures coherent combining of the data samples spread over the Doppler-frequency grid and non-coherent combining of inter-carrier interference (ICI) components caused by time varying fading. Theoretical error probabilities of the OOFDM systems are derived by analyzing the statistical properties of Doppler-frequency fading coefficients and noise sample correlations. Both theoretical analysis and computer simulation show that the new system with an oversampling factor of two outperforms the conventional OFDM system by as much as 7 dB.

**Index Terms**—OFDM, oversampled OFDM, multipath diversity, Doppler diversity, ICI.

## I. INTRODUCTION

ORTHOGONAL frequency division multiplexing (OFDM) has emerged as the leading transmission technique for a wide range of wireless and wireline communication standards [1]. The conventional OFDM system is designed primarily for static or quasi-static channels, where the channel response remains constant for at least one symbol period [2] – [4]. However, high mobility broadband communication dictates an operating environment of doubly selective (both time selective and frequency selective) fading. Time selective fading introduces severe Doppler spread that destroys subcarrier orthogonality and causes inter-carrier interference (ICI) [5]. Various signal processing techniques, such as Doppler domain equalization [6] – [8], precoding [2] and [9], or time-frequency localization [10], have been developed to suppress the impairments caused by ICI.

Doubly selective fading, if handled properly, can also be exploited to benefit the OFDM system design to collect diversity gains. Doppler spread caused by fading time variation

introduces Doppler diversity [11], [12]; while time dispersion due to frequency selective fading leads to multipath diversity [2] – [4]. OFDM systems are inherently superior to single carrier systems in terms of Doppler diversity thanks to its longer symbol period [12]. On the other hand, no multipath diversity can be achieved by conventional uncoded OFDM systems, because uncorrelated narrow band data streams are transmitted at different subcarriers [4]. So far, most works in the literature resort to linear precoding/decoding or zero-padding in OFDM to achieve multipath diversity, at the cost of spectral efficiency and/or system complexity [2] – [4].

Time domain oversampling, or fractionally spaced sampling, has been extensively studied for single carrier systems [13] – [15]. However, very limited works on fractionally spaced receiver are available for multicarrier systems [16] – [20]. In OFDM systems, time domain oversampling has been used mainly as a tool to facilitate the analysis of peak to average power ratio (PAPR) of the time domain OFDM signals [16]. In [17] and [18], the oversampled OFDM signals are used to assist the blind estimation of quasi-static fading channels. Recently, it has been shown in [19] that fractionally spaced sampling of the time domain OFDM signal leads to potential multipath diversity. In [20], additional signal-to-noise ratio (SNR) gain in oversampled OFDM system is achieved by extending the oversampling factor from integers to rational numbers. All of the aforementioned works are only applicable to OFDM systems in quasi-static fading channels.

In this paper, we propose a new oversampled OFDM (OOFDM) receiver structure for both quasi-static and doubly selective fading channels. The proposed OOFDM system employs oversampling in the time domain and linear processing in the frequency domain. We develop a new system model with an equivalent two dimensional (2D) representation: the frequency response due to time varying fading is denoted as the Doppler domain, and the frequency response due to frequency selective fading as the frequency domain. The new Doppler-frequency representation enables a new channel model of the OOFDM system, where each data symbol is treated as if it is transmitted over multiple subcarriers and various Doppler spreads simultaneously. Based on the new channel model, optimum and sub-optimum receivers are developed to perform coherent combining of the received data samples spread over the Doppler-frequency grid, and this simultaneously harvests the multipath diversity and Doppler diversity inherent in doubly selective fading channels. At the mean time, coherent combining of the data samples renders non-coherent combining of ICI components, therefore achieving better symbol error performance than conventional OFDM systems. Theoretical

Paper approved by E. Perrins, the Editor for Modulation Theory of the IEEE Communications Society. Manuscript received October 30, 2009; revised June 18, 2010.

J. Wu is with the Department of Electrical Engineering, University of Arkansas, Fayetteville, AR 72701, USA (e-mail: wuj@uark.edu).

Y. R. Zheng is with the Department of Electrical and Computer Engineering, Missouri University of Science and Technology, Rolla, MO 65409, USA (e-mail: zhengyr@mst.edu).

Digital Object Identifier 10.1109/TCOMM.2011.121410.090655

error probability expressions of the proposed OOFDM system are derived by analyzing the statistical properties of Doppler-frequency channel coefficients and noise sample correlations.

In the remainder of this paper, the OOFDM system model is described in Section II. Section III proposes a Doppler-frequency domain linear receiver. An optimum receiver for the OOFDM system in quasi-static frequency selective fading is presented in Section IV. The optimum OOFDM receiver for doubly selective fading channel is computationally expensive. Therefore, a sub-optimum receiver employing block decision feedback equalization (BDFE) is proposed in Section V. Simulation results are given in Section VI, and Section VII concludes the paper.

Throughout the paper, the superscripts  $(\cdot)^T$  and  $(\cdot)^H$  denote matrix transpose and Hermitian, respectively. The superscript  $(\cdot)^*$  denotes the conjugate. The complex matrix space of size  $M \times N$  is denoted as  $\mathcal{C}^{M \times N}$ , and  $\mathbb{E}(\cdot)$  denotes the mathematical expectation. The modulation constellation set is denoted as  $\mathcal{S}$ .

## II. SYSTEM MODEL

The baseband representation of the new OOFDM structure is shown in Fig. 1, where the baseband equivalent channel impulse response (CIR) of the doubly selective fading channel,  $c(t, \tau)$ , can be viewed as the response of the channel at time  $t$  to an impulse input at time  $t - \tau$ . At the transmitter, a block of  $N$  data symbols,  $\mathbf{s} = [s(0), \dots, s(N-1)]^T \in \mathcal{S}^{N \times 1}$ , are modulated onto  $N$  orthogonal subcarriers through the basis functions  $\phi_n(t) = \frac{1}{\sqrt{N}} e^{j2\pi n F_0 t}$ , for  $0 \leq t \leq T_0$  and  $n = 0, \dots, N-1$ , where  $F_0 = \frac{1}{T_0}$  is the subcarrier spacing, and  $T_0$  is the duration of one OFDM symbol. The multicarrier modulated signal,  $x(t) = \sum_{n=0}^{N-1} s(n) \phi_n(t)$ , are sampled at the transmitter at a sampling period of  $T_1 = \frac{T_0}{N}$ , which yields  $N$  time domain samples,  $\mathbf{x} = [x(0), x(1), \dots, x(N-1)]^T$ , per symbol period. The resulting time domain samples can be viewed as the inverse discrete Fourier transform (IDFT) of  $\mathbf{s}$  as  $\mathbf{x} = \mathbf{F}_N^H \mathbf{s}$ , where  $\mathbf{F}_N \in \mathcal{C}^{N \times N}$  is the normalized  $N$ -point discrete Fourier transform (DFT) matrix with the  $(m, n)$ -th element being  $(\mathbf{F}_N)_{m,n} = \frac{1}{\sqrt{N}} \exp[-j2\pi \frac{(m-1)(n-1)}{N}]$ .

Cyclic prefix are inserted in the time domain to avoid inter-block interference. The prefixed time domain samples are passed through a transmit filter,  $p_1(t)$ , and then transmitted to the channel. At the receiver, the received signal is passed through a receive filter,  $p_2(t)$ . Define the continuous-time composite impulse response of the channel as  $g(t, \tau) = p_1(\tau) \odot c(t, \tau) \odot p_2(\tau)$ , where  $a(\tau) \odot b(t, \tau) = \int b(t, \alpha) a(\tau - \alpha) d\alpha$  representing the convolution of time varying signals. The time variation of the channel follows a Doppler spectrum. The received time domain signal can then be represented as

$$y(t) = \sum_{n=-\infty}^{+\infty} x(n)g(t, t - nT_1) + z(t), \quad (1)$$

where  $z(t) = p_2(t) \odot v(t)$  is the noise component at the output of the receive filter, with  $v(t)$  being additive white Gaussian noise (AWGN) with variance  $N_0$ , and  $x(n)$  is the cyclic-prefixed time domain samples with a sample period  $T_1$ .

The output of the receive filter is sampled at the time instant  $t = nT_2$ , where  $T_2 = T_1/u$  is the sampling period at the

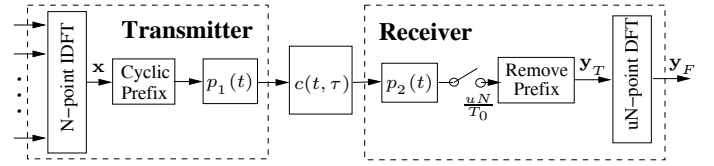


Fig. 1. The block diagram of the proposed oversampled OFDM system.

receiver, with the oversampling factor,  $u$ , being an integer. The sampled output is

$$y_T(n) = \sum_{l=0}^{uL-1} x_T(n-l)g_T(n, l) + z_T(n), \quad n = 0, \dots, uN-1. \quad (2)$$

where  $y_T(n) = y(nT_2)$  and  $z_T(n) = z(nT_2)$  are the  $T_2$ -spaced samples of the received signals and noise, respectively, and  $g_T(n, l) = g(nT_2, lT_2)$  is the discrete-time CIR with  $uL$  channel taps at  $T_2$ -spacing. The channel length of the oversampled discrete-time CIR is assumed to be an integer multiple of the oversampling factor  $u$ . This condition can always be met by padding zeros to the CIR. The subscript  $(\cdot)_T$  denotes  $T_2$ -spaced time domain samples, and  $x_T(n)$  is the oversampled version of  $x(n)$  as  $x_T(n) = x(n/u)$ , if  $n/u$  is an integer, and 0 otherwise.

It is assumed that the receiver has perfect knowledge of the discrete-time CIR,  $g_T(n, l)$ . The system equation in (2) can also be represented in a matrix format as

$$\mathbf{y}_T = \mathbf{G}_T \mathbf{x} + \mathbf{z}_T, \quad (3)$$

where  $\mathbf{y}_T = [y_T(0), \dots, y_T(uN-1)]^T \in \mathcal{C}^{uN \times 1}$ ,  $\mathbf{z}_T = [z_T(0), \dots, z_T(uN-1)]^T \in \mathcal{C}^{uN \times 1}$ , and  $\mathbf{G}_T = [\mathbf{g}_1, \mathbf{g}_{u+1}, \mathbf{g}_{2u+1}, \dots, \mathbf{g}_{(N-1)u+1}] \in \mathcal{C}^{uN \times N}$ , with  $\mathbf{g}_k \in \mathcal{C}^{uN \times 1}$  being the  $k$ -th column of the matrix  $\mathbf{G}$  defined in (4).

The system performance depends on the properties of the discrete-time CIR,  $g_T(n, l)$ , and noise sample,  $z_T(n)$ . The statistical properties of  $g_T(n, l)$  and  $z_T(n)$  are summarized in the following two Lemmas [21].

*Lemma 1:* For a channel undergoing wide sense stationary uncorrelated scattering (WSSUS) time varying and frequency selective fading, the discrete time CIR,  $g_T(n, l)$ , is zero-mean complex Gaussian distributed with covariance given by

$$\mathbb{E}[g_T(n_1, l_1)g_T^*(n_2, l_2)] = J_0[2\pi F_d(n_1 - n_2)T_2] \rho(l_1, l_2), \quad (5)$$

where  $J_0(x)$  is the zero-order Bessel function of the first kind,  $F_d$  is the maximum Doppler spread, and  $\rho(l_1, l_2)$  represents the correlation between the channel taps, with

$$\rho(l_1, l_2) = \int_{-\infty}^{+\infty} R_{p_1 p_2}(l_1 T_2 - \mu) R_{p_1 p_2}^*(l_2 T_2 - \mu) G(\mu) d\mu, \quad (6)$$

where  $R_{p_1 p_2}(t) = p_1(t) \odot p_2(t)$ , and  $G(\mu)$  is the normalized channel power delay profile with  $\int_{-\infty}^{+\infty} G(\mu) d\mu = 1$ . ■

*Lemma 2:* The time domain noise vector,  $\mathbf{z}_T$ , is zero-mean complex Gaussian distributed with a covariance matrix  $\mathbf{R}_{z_T} = \mathbb{E}(\mathbf{z}_T \mathbf{z}_T^H) = N_0 \mathbf{R}_p$ , where  $N_0$  is the variance of AWGN. The  $(m, n)$ -th element of the matrix  $\mathbf{R}_p \in \mathcal{C}^{uN \times uN}$  is  $(\mathbf{R}_p)_{m,n} = R_{p_2 p_2}(m - n)$ , where  $R_{p_2 p_2}(n) = \int_{-\infty}^{+\infty} p_2(nT_2 + \tau) p_2(\tau) d\tau$  is the autocorrelation function of the receive filter,  $p_2(t)$ . ■

$$\mathbf{G} = \begin{pmatrix} g_T(0,0) & 0 & \cdots & g_T(0,uL-1) & \cdots & g_T(0,1) \\ g_T(1,1) & g_T(1,0) & \cdots & 0 & g_T(1,uL-1) & \cdots \\ \vdots & \ddots & \ddots & \ddots & \ddots & \vdots \\ 0 & \cdots & g_T(uN-1,uL-1) & \cdots & \cdots & g_T(uN-1,0) \end{pmatrix} \in \mathcal{C}^{uN \times uN}. \quad (4)$$

Due to the time dispersion of  $p_1(t)$  and  $p_2(t)$ , the discrete-time channel taps,  $g_T(n, l)$ , are mutually correlated in both the time domain,  $n$ , and the delay domain,  $l$ , even though the underlying fading channel experiences uncorrelated scattering. Likewise, the noise samples,  $z_T(n)$ , are correlated with their correlation coefficients determined by the receive filter,  $p_2(t)$ .

Since the noise elements are mutually correlated, the noise covariance matrix,  $\mathbf{R}_{z_T}$ , might be rank deficient. Define the pseudo-inverse of  $\mathbf{R}_{z_T}$  as

$$\mathbf{R}_{z_T}^\dagger = \frac{1}{N_0} \mathbf{V}_p \mathbf{\Omega}_p^{-1} \mathbf{V}_p^H, \quad (7)$$

with

$$\mathbf{V}_p = [\mathbf{v}_{p1}, \mathbf{v}_{p2}, \cdots, \mathbf{v}_{pu_p}] \in \mathcal{C}^{uN \times u_p}, \quad (8a)$$

$$\mathbf{\Omega}_p = \text{diag}[\omega_{p1}, \omega_{p2}, \cdots, \omega_{pu_p}] \in \mathcal{C}^{u_p \times u_p} \quad (8b)$$

where  $u_p$  is the number of non-zero eigenvalues of  $\mathbf{R}_p$ ,  $\mathbf{\Omega}_p$  is a diagonal matrix, with the diagonal elements,  $\{\omega_{pi}\}_{i=1}^{u_p}$ , being the non-zero eigenvalues of  $\mathbf{R}_p$ , and  $\{\mathbf{v}_{pi}\}_{i=1}^{u_p}$  are the corresponding orthonormal eigenvectors.

With the pseudo-inverse matrix defined in (7), the optimum maximum likelihood (ML) receiver of the OOFDM system is

$$\hat{\mathbf{s}} = \underset{\mathbf{s} \in \mathcal{S}^N}{\text{argmin}} (\mathbf{y}_T - \mathbf{G}_T \mathbf{F}_N^H \mathbf{s})^H \mathbf{V}_p \mathbf{\Omega}_p^{-1} \mathbf{V}_p^H (\mathbf{y}_T - \mathbf{G}_T \mathbf{F}_N^H \mathbf{s}), \quad (9)$$

where  $\mathcal{S}^N$  is the set containing all the possible vectors of  $\mathbf{s}$  with cardinality  $M^N$ , with  $M$  being the modulation level and  $N$  the number of symbols per block. The optimum receiver in (9) performs exhaustive search in the signal space, and it can fully collect the multipath diversity and Doppler diversity inherent in the channel matrix,  $\mathbf{G}_T$ , which completely characterizes the OOFDM system.

### III. DOPPLER-FREQUENCY DOMAIN LINEAR RECEIVER

In this section, a linear receiver is presented to convert the original OFDM system with  $N$  subcarriers into an equivalent system with  $uN$  subcarriers. In addition, the linear receiver enables separate control over the Doppler domain and the frequency domain.

Due to the higher sampling rate at the receiver, there are  $uN$  time domain samples after the removal of the cyclic prefix. Performing the  $uN$ -point DFT over the time domain sample vector  $\mathbf{y}_T$  in (3), we have

$$\mathbf{y}_F = \mathbf{G}_F \mathbf{s} + \mathbf{z}_F, \quad (10)$$

where  $\mathbf{y}_F = \mathbf{F}_{uN} \mathbf{y}_T = [y_F(0), \cdots, y_F(uN-1)]^T$  and  $\mathbf{z}_F = \mathbf{F}_{uN} \mathbf{z}_T = [z_F(0), \cdots, z_F(uN-1)]^T$  are the frequency domain sample vector and noise vector, respectively, and  $\mathbf{G}_F = \mathbf{F}_{uN} \mathbf{G}_T \mathbf{F}_N^H \in \mathcal{C}^{uN \times N}$ .

*Proposition 1:* Partition the matrix  $\mathbf{G}_F$  into a stack of  $u$  sub-matrices as  $\mathbf{G}_F = [\mathbf{H}_0^T, \cdots, \mathbf{H}_{u-1}^T]^T$ , where  $\mathbf{H}_m \in$

$\mathcal{C}^{N \times N}$ . The  $(i, k)$ -th element of  $\mathbf{H}_m$  is the discrete Doppler-frequency transfer function,  $g_{DF}(\frac{i-k}{uN}, \frac{mN+k-1}{uN})$ , defined as

$$g_{DF}(d, f) = \frac{1}{\sqrt{uN}} \sum_{v=0}^{u-1} \sum_{n=0}^{N-1} \sum_{l=0}^{L-1} g_T(un+v, ul+v) \times e^{-j2\pi(ul+v)d} e^{-j2\pi(un+v)f} \quad (11)$$

*Proof:* The  $(i, k)$ -th element of  $\mathbf{H}_m$  is the  $(mN+i, k)$ -th element of  $\mathbf{G}_F$ . Based on the definition of  $\mathbf{G}_T$  and  $\mathbf{G}_F$ , the  $(i, k)$ -th element of  $\mathbf{H}_m$  can be calculated by

$$(\mathbf{H}_m)_{i,k} = \frac{1}{\sqrt{uN}} \sum_{q=0}^{uN-1} e^{-j2\pi \frac{(mN+i-1)q}{uN}} \sum_{l=0}^{L-1} g_T(q, q+ul) e^{-j2\pi \frac{(k-1)l}{N}}.$$

Let  $q = un + v$  for  $n = 0, \cdots, N-1$  and  $v = 0, \cdots, u-1$ ,

$$(\mathbf{H}_m)_{i,k} = \frac{1}{\sqrt{uN}} \sum_{n=0}^{N-1} \sum_{v=0}^{u-1} e^{-j2\pi \frac{(mN+i-1)(un+v)}{uN}} \sum_{l_1=0}^{L-1} g_T(un+v, ul_1+v) e^{-j2\pi \frac{(k-1)(l_1-n)}{N}}. \quad (12)$$

where  $l_1 = l + n$ . Eqn. (11) can then be obtained by combining (12) with the identity  $e^{-j2\pi \frac{(k-1)l}{N}} = e^{-j2\pi \frac{(mN+k-1)l}{uN}}$ . ■

The Doppler-frequency transfer function,  $g_{DF}(d, f)$ , is obtained from the double discrete-time Fourier transform of the time varying discrete-time CIR,  $g_T(n, l)$ . In  $g_{DF}(d, f)$ , the variable  $d$  is the index of Doppler spread due to fading time variation, and  $f$  represents frequency response from fading dispersion. We denote  $d$  as the Doppler domain, and  $f$  as the frequency domain. It should be noted that the conventional OFDM system does not distinguish the Doppler domain from the frequency domain. However, these two domains have completely different properties due to their different causes.

The result in Proposition 1 leads to an equivalent Doppler-frequency system representation with channel coefficients,  $g_{DF}(\frac{i}{uN}, \frac{k}{uN})$ , for  $i = 0, \cdots, uN-1$ , and  $k = 0, \cdots, uN-1$ . In the new system, the space between two adjacent indices in both the Doppler and the frequency domain is  $\frac{1}{uNT_2} = \frac{1}{NT_1} = \frac{1}{T_0}$ , which is the same as conventional OFDM systems. However, the supports in the two domain are expanded to  $[0, \frac{uN}{T_0}]$ . With  $uN$  indices in the frequency domain support, there are totally  $uN$  subcarriers in the equivalent system, with the  $(k+1)$ -th diagonal element of  $\mathbf{H}_m$ ,  $g_{DF}(0, \frac{mN+k}{uN})$ , being the coefficient of the  $(mN+k)$ -th subcarrier. Thus the receiver oversampling in the time domain converts the original  $N$ -subcarrier system into an equivalent system with  $uN$  subcarriers. From (10), each modulated data symbol,  $s(k)$ , is equivalently transmitted over  $u$  subcarriers with channel coefficients  $\{g_{DF}(0, \frac{mN+k}{uN})\}_{m=0}^{u-1}$ . Thus multipath diversity is achieved in the proposed OOFDM system due to the expansion of the frequency domain support.

The non-diagonal elements of  $\mathbf{H}_m$  are due to the Doppler spread of the time varying channel. They introduce both ICI and Doppler diversity. Specifically, the  $(i, k)$ -th element of  $\mathbf{H}_m$ ,  $g_{DF}\left(\frac{i-k}{uN}, \frac{mN+k-1}{uN}\right)$ , is determined by the Doppler spread at  $\frac{i-k}{T_0}$ . On the  $(mN+k)$ -th subcarrier, the data symbol,  $s(k)$ , is transmitted over  $N$  different Doppler spreads, as represented by  $\left\{g_{DF}\left(\frac{i-k}{uN}, \frac{mN+k}{uN}\right)\right\}_{i=0}^{N-1}$ . As a result, Doppler diversity can be achieved via coherent combining of signal components and non-coherent combining of the interference and noise components.

From the analysis above, each data symbol,  $s(k)$ , is transmitted over a 2D Doppler-frequency grid formulated by  $u \times N$  channel coefficients,  $g_{DF}\left(\frac{i-k}{uN}, \frac{mN+k}{uN}\right)$ , for  $m = 0, 1, \dots, u-1$  and  $i = 0, 1, \dots, N-1$ . Therefore, both multipath diversity and Doppler diversity are achieved simultaneously in the OOFDM system by means of spreading data over the 2D Doppler-frequency grid.

In the next two sections, two diversity receivers are presented for quasi-static frequency selective fading and doubly selective fading channels, respectively.

#### IV. OPTIMUM COMBINING FOR OOFDM IN QUASI-STATIC FADING CHANNELS

An optimum OOFDM diversity receiver is presented in this section to collect the multipath diversity in a quasi-static frequency selective fading channel.

For the special case of quasi-static fading,  $g_T(n, l)$  degrades to  $g_T(l)$ . Correspondingly, the frequency response matrix,  $\mathbf{H}_m$ , degrades to a diagonal matrix with the properties specified in the following corollary.

*Corollary 1:* For a quasi-static frequency selective fading channel, the matrix,  $\mathbf{H}_m$ , is a diagonal matrix, with the diagonal elements obtained from the  $uN$ -point DFT of the discrete-time CIR, up to a scaling factor. The  $k$ -th diagonal element of  $\mathbf{H}_m$  can be written as

$$h_m(k) \triangleq (\mathbf{H}_m)_{k,k} = \frac{1}{\sqrt{u}} \sum_{l=0}^{uL-1} g_T(l) e^{-j2\pi \frac{(mN+k-1)l}{uN}}, \quad (13)$$

where  $g_T(l)$ , for  $l = 0, \dots, uL-1$ , is the time-invariant discrete-time CIR of the frequency selective fading.

*Proof:* From (12), the  $(i, k)$ -th element of  $\mathbf{H}_m$  in a quasi-static channel can be calculated by

$$(\mathbf{H}_m)_{i,k} = \frac{1}{\sqrt{uN}} \sum_{v=0}^{u-1} \sum_{l_1=0}^{L-1} \sum_{n=0}^{N-1} g_T(ul_1 + v) \times e^{-j2\pi \frac{(mN+k-1)(ul_1+v)}{uN}} e^{-j2\pi \frac{(i-k)(un+v)}{uN}}. \quad (14)$$

When  $i = k$ , it can be easily shown that  $(\mathbf{H}_m)_{k,k} = \frac{1}{\sqrt{u}} \sum_{v=0}^{u-1} \sum_{l_1=0}^{L-1} g_T(ul_1 + v) e^{-j2\pi \frac{(mN+k-1)(ul_1+v)}{uN}}$ , which is equivalent to (13) by letting  $l = ul_1 + v$ . When  $i \neq k$ , (14) can be written as  $(\mathbf{H}_m)_{i,k} = \frac{1}{\sqrt{uN}} a_{i,k} \sum_{n=0}^{N-1} e^{-j2\pi \frac{(i-k)n}{N}} = 0$ , where  $a_{i,k} = \sum_{v=0}^{u-1} \sum_{l_1=0}^{L-1} g_T(ul_1+v) e^{-j2\pi \frac{(mN+k-1)(ul_1+v)}{uN}} e^{-j2\pi \frac{(i-k)v}{uN}}$ . ■

#### A. Optimum Combining

For the quasi-static fading channel model, the diagonal elements of  $\mathbf{H}_m$  is directly obtained from the  $uN$ -point DFT of the discrete-time CIR, and this leads to a total of  $uN$  subcarriers with  $h_m(k)$  being the coefficient of the  $(mN+k)$ -th subcarrier. Therefore, each data symbol of the OOFDM system is equivalently transmitted over  $u$  subcarriers experiencing no ICI. Stacking all the  $u$  subcarriers related to the symbol  $s(k)$  leads to an alternative single input multiple output (SIMO) system model

$$\mathbf{r}(k) = \mathbf{h}(k) \cdot s(k) + \mathbf{w}(k), \quad \text{for } k = 0, \dots, N-1, \quad (15)$$

where  $\mathbf{r}(k) = [r_0(k), r_1(k), \dots, r_{u-1}(k)]^T$  with  $r_m(k) = y_F(mN+k)$ ,  $\mathbf{h}(k) = [h_0(k), h_1(k), \dots, h_{u-1}(k)]^T$ , and  $\mathbf{w}(k) = [w_0(k), w_1(k), \dots, w_{u-1}(k)]^T$  with  $w_m(k) = z_F(mN+k)$ .

*Corollary 2:* For an OOFDM system in quasi-static frequency selective Rayleigh fading and AWGN, the frequency domain vectors,  $\mathbf{h}(k)$  and  $\mathbf{w}(k)$ , are zero mean complex Gaussian distributed with their respective covariance matrices,  $\mathbf{R}_h^{(k)} = \mathbb{E}[\mathbf{h}(k)\mathbf{h}^H(k)]$ , and  $\mathbf{R}_w^{(k)} = \mathbb{E}[\mathbf{w}(k)\mathbf{w}^H(k)]$ , given by

$$\mathbf{R}_h^{(k)} = N \cdot \mathbf{F}_{uN}(k) \cdot \mathbf{R}_{g_T} \cdot \mathbf{F}_{uN}^H(k), \quad (16a)$$

$$\mathbf{R}_w^{(k)} = N_0 \cdot \mathbf{F}_{uN}(k) \cdot \mathbf{R}_p \cdot \mathbf{F}_{uN}^H(k). \quad (16b)$$

where  $\mathbf{R}_p \in \mathcal{C}^{uN \times uN}$  is defined in Lemma 2, and  $\mathbf{F}_{uN}(k) \in \mathcal{C}^{u \times uN}$  is obtained by extracting a subset of  $u$  rows from the normalized  $uN$ -point DFT matrix, with the  $(m, n)$ -th element of  $\mathbf{F}_{uN}(k)$  being  $\frac{1}{\sqrt{uN}} e^{-j2\pi \frac{(m-1)N+k(n-1)}{uN}}$ . The time domain channel covariance matrix  $\mathbf{R}_{g_T} \in \mathcal{C}^{uN \times uN}$  is defined with its  $(m, n)$ -th element being  $(\mathbf{R}_{g_T})_{m,n} = \rho(m-1, n-1)$ , for  $1 \leq m, n \leq uL$  and 0 otherwise.

*Proof:* From (13) and the definition of  $\mathbf{z}_F$ , we have  $\mathbf{h}(k) = \sqrt{N} \cdot \mathbf{F}_{uN}(k) \cdot \mathbf{g}_T$ , and  $\mathbf{w}(k) = \mathbf{F}_{uN}(k) \cdot \mathbf{z}_T$ , where  $\mathbf{g}_T = [g_T(0), \dots, g_T(uL-1), 0, \dots, 0]^T \in \mathcal{C}^{uN \times 1}$  is the time domain discrete-time CIR vector. Combining the above equations with Lemmas 1 and 2 leads to (16). ■

The results in (16) indicate that the SIMO system of (15) has correlated channel taps and is corrupted by a colored noise. The covariance matrix,  $\mathbf{R}_w^{(k)}$ , of the colored noise might be rank deficient. To facilitate the analysis, define the pseudo-inverse of  $\frac{1}{N_0} \mathbf{R}_w^{(k)}$  as

$$\Phi_k = \mathbf{V}_k \mathbf{\Omega}_k^{-1} \mathbf{V}_k^H \in \mathcal{C}^{u \times u}, \quad (17)$$

with  $\mathbf{V}_k = [\mathbf{v}_{k1}, \mathbf{v}_{k2}, \dots, \mathbf{v}_{ku_w}] \in \mathcal{C}^{uN \times u_w}$ , and  $\mathbf{\Omega}_k = \text{diag}[\omega_{k1}, \omega_{k2}, \dots, \omega_{ku_w}] \in \mathcal{C}^{u_w \times u_w}$  being the reduced eigenvector matrix and eigenvalue matrix of  $\frac{1}{N_0} \mathbf{R}_w^{(k)}$ , respectively, and  $u_w$  is the rank of  $\mathbf{R}_w^{(k)}$ . With the pseudo-inverse matrix defined in (17), the optimum diversity receiver for the equivalent SIMO system is described by the following proposition.

*Proposition 2:* The optimum decision rule for the SIMO system described in (15) is

$$\hat{s}(k) = \underset{s(k) \in \mathcal{S}}{\text{argmax}} |\varphi_k - q_k s(k)|^2 \quad (18)$$

where  $q_k = \mathbf{h}^H(k) \Phi_k \mathbf{h}(k)$ , and  $\varphi_k = \mathbf{h}^H(k) \Phi_k \mathbf{r}(k)$ .

*Proof:* Define the noise whitening matrix as  $\mathbf{D}_k = \mathbf{\Omega}_k^{-\frac{1}{2}} \mathbf{V}_k^H$ . Applying  $\mathbf{D}_k$  to both sides of (15) leads to

$$\bar{\mathbf{r}}(k) = \bar{\mathbf{h}}(k) \cdot s(k) + \bar{\mathbf{w}}(k), \quad (19)$$

where  $\bar{\mathbf{r}}(k) = \mathbf{D}_k \mathbf{r}(k)$ ,  $\bar{\mathbf{h}}(k) = \mathbf{D}_k \mathbf{h}(k)$ , and  $\bar{\mathbf{w}}(k) = \mathbf{D}_k \mathbf{w}(k)$  with the covariance matrix of  $\bar{\mathbf{w}}(k)$  being  $\mathbf{R}_{\bar{\mathbf{w}}} = N_0 \mathbf{I}_{u_p}$ . Applying maximal ratio combining (MRC) to (19), i.e.,  $\varphi_k = \bar{\mathbf{h}}^H(k) \bar{\mathbf{r}}(k)$ , leads to the optimum decision rule in (18). ■

## B. Performance Analysis

The exact symbol error rate (SER) of the OOFDM system with the optimum diversity receiver described in Proposition 2 is derived in this subsection.

Combining (15) and Proposition 2 yields an alternative representation of the decision variable as  $\varphi_k = q_k \cdot s(k) + \mathbf{h}^H(k) \mathbf{\Phi}_k \mathbf{w}(k)$ . Thus, the SNR at the output of the optimum receiver is

$$\gamma_k = \frac{|q_k|^2 E_s}{\mathbf{h}^H(k) \mathbf{\Phi}_k \mathbf{R}_{\mathbf{w}}(k) \mathbf{\Phi}_k^H \mathbf{h}(k)} = q_k \gamma_0, \quad (20)$$

where  $\gamma_0 = E_s/N_0$  is the SNR without fading, with  $E_s$  being the energy of one symbol. Based on the SNR  $\gamma_k$ , the SER of the  $k$ -th data stream for linear modulation schemes, such as M-ary amplitude shift keying (MASK), M-ary phase shift keying (MPSK), and M-ary quadrature amplitude modulation (MQAM), can be written in a unified expression as [15]

$$P(E_k) = \sum_{i=1}^2 \frac{\beta_i}{\pi} \int_0^{\psi_i} \prod_{i=1}^{\tilde{u}_k} \left( 1 + \zeta \gamma_0 \cdot \frac{\lambda_i}{\sin^2 \theta} \right)^{-1} d\theta, \quad (21)$$

where  $\tilde{u}_k$  is the rank of the product matrix,  $\mathbf{R}_h^{(k)} \mathbf{\Phi}_k$ , with  $\lambda_i$  being the corresponding non-zero eigenvalues, and the values of  $\zeta$ ,  $\beta_i$ , and  $\psi_i$  for the various modulation schemes can be found in [15, Table 1]. With  $P(E_k)$  given in (21), the exact SER for the OOFDM system in quasi-static fading channels can then be calculated as  $P(E) = \frac{1}{N} \sum_{k=0}^{N-1} P(E_k)$ .

It's apparent from (21) that the multipath diversity order of the OOFDM is equal to the rank of the product matrix,  $\mathbf{R}_h^{(k)} \mathbf{\Phi}_k$ , which is in turn determined by the time domain covariance matrices,  $\mathbf{R}_{g_T}$  and  $\mathbf{R}_p$ .

## V. DOPPLER DOMAIN EQUALIZATION FOR OOFDM IN DOUBLY SELECTIVE FADING

A Doppler domain equalizer is presented in this section to simultaneously collect the Doppler diversity and mitigate the ICI impairments caused by the fading time variation.

### A. Doppler Domain Equalization

In a doubly selective fading channel, each data symbol,  $s(k)$ , is transmitted over a  $u \times N$  Doppler-frequency grid defined by  $g_{DF} \left( \frac{i-k}{uN}, \frac{mN+k}{uN} \right)$ , for  $m = 0, \dots, u-1$  and  $i = 0, \dots, N-1$ , as shown in (10) and Proposition 1. The Doppler-frequency system representation in (10) is an equivalent multiple-input multiple-output (MIMO) system with  $N$  inputs,  $\mathbf{s}$ , and  $uN$  outputs,  $\mathbf{y}_F$ . Due to the correlation among

noise samples in the time domain, the elements of the frequency domain noise vector,  $\mathbf{z}_F$ , are also correlated. Based on Lemma 2, the covariance matrix of  $\mathbf{z}_F$  is

$$\mathbf{R}_{\mathbf{z}_F} = N_0 \cdot \mathbf{F}_{uN} \mathbf{R}_p \mathbf{F}_{uN}^H. \quad (22)$$

Since the noise elements are mutually correlated, the noise covariance matrix,  $\mathbf{R}_{\mathbf{w}}$ , might be rank deficient. Define the pseudo-inverse of  $\frac{1}{N_0} \mathbf{R}_{\mathbf{w}}$  as

$$\mathbf{\Phi} = \mathbf{F}_{uN} \mathbf{V}_p \mathbf{\Omega}_p^{-1} \mathbf{V}_p^H \mathbf{F}_{uN}^H, \quad (23)$$

where the reduced eigenvector matrix,  $\mathbf{V}_p$ , and the reduced eigenvalue matrix,  $\mathbf{\Omega}_p$ , are defined in (8).

From (23), define noise whitening matrix  $\mathbf{D} = \frac{1}{\sqrt{u}} \mathbf{\Omega}_p^{-1/2} \mathbf{V}_p^H \mathbf{F}_{uN}^H \in \mathcal{C}^{u_p \times uN}$ . Multiplying  $\mathbf{D}$  on both sides of (10) leads to an equivalent system

$$\bar{\mathbf{r}} = \bar{\mathbf{H}} \mathbf{s} + \bar{\mathbf{w}}, \quad (24)$$

where  $\bar{\mathbf{r}} = \mathbf{D} \mathbf{y}_F$ ,  $\bar{\mathbf{H}} = \mathbf{D} \mathbf{G}_F$ , and  $\bar{\mathbf{w}} = \mathbf{D} \mathbf{z}_F$ . The covariance matrix of the noise vector,  $\bar{\mathbf{w}}$ , in the equivalent system can be calculated as  $\mathbf{R}_{\bar{\mathbf{w}}} = \mathbf{D} \mathbf{R}_{\mathbf{z}_F} \mathbf{D}^H = N_0 \mathbf{I}_{u_p}$ . Therefore, the original MIMO system in (10) with  $uN$  outputs and a colored noise is converted to an equivalent MIMO system with  $u_p$  outputs and a white noise.

Based on (24), the optimum maximum likelihood decision rule of the system can be described as

$$\hat{\mathbf{s}} = \underset{\mathbf{s} \in \mathcal{S}^N}{\text{argmax}} (\bar{\mathbf{r}} - \bar{\mathbf{H}} \mathbf{s})^H (\bar{\mathbf{r}} - \bar{\mathbf{H}} \mathbf{s}). \quad (25)$$

The optimum solution in (25) can be obtained through exhaustive search with a complexity on the order of  $\mathcal{O}(M^N)$ , which is often prohibitive for practical systems with large values of  $M$  and/or  $N$ . To simplify the operation, a sub-optimum Doppler domain block decision feedback equalizer (DD-BDFE) is developed. The DD-BDFE scheme contains two filters, a feed forward filter,  $\mathbf{A} \in \mathcal{C}^{N \times u_p}$ , and an upper triangular filter with unit diagonal elements as the feedback filter,  $\mathbf{B} \in \mathcal{C}^{N \times N}$ . Based on the assumption of correct past detection, the error vector,  $\mathbf{e}$ , of the BDFE can be expressed by  $\mathbf{e} = \mathbf{A} \bar{\mathbf{r}} - \mathbf{B} \mathbf{s}$ . Based on the minimum mean square error (MMSE) criterion,  $\mathbf{B}$  can be obtained from the Cholesky decomposition [22]

$$\frac{1}{E_s} \mathbf{I}_N + \bar{\mathbf{H}}^H \mathbf{\Phi} \bar{\mathbf{H}} = \mathbf{B}^H \mathbf{\Lambda} \mathbf{B} \quad (26)$$

with  $\mathbf{\Lambda}$  being a diagonal matrix. The feedforward matrix,  $\mathbf{A}$ , can then be calculated as

$$\mathbf{A} = \mathbf{B} \bar{\mathbf{H}}^H \left[ \bar{\mathbf{H}} \bar{\mathbf{H}}^H + \frac{1}{\gamma_0} \mathbf{I}_{u_p} \right]^{-1}. \quad (27)$$

Since  $\mathbf{B}$  is upper triangular, the  $(m, n)$ -th element of  $\mathbf{B}$ ,  $b_{mn}$ , satisfies  $b_{mn} = 0, \forall n < m$ . Therefore, the information symbols are detected in a reverse order, i.e.,  $s(N-1)$  is detected first and  $s(0)$  is detected last within one OFDM symbol. The output of the BDFE equalizer can then be described as

$$\hat{s}(n) = \underset{s(n) \in \mathcal{S}}{\text{argmin}} \left| \bar{r}(n) - b_{n,n} s(n) - \sum_{m=n+1}^{N-1} b_{n,m} \hat{s}(m) \right|^2, n=0, \dots, N-1.$$

where  $\bar{r}(n)$  is the  $n$ -th element of  $\bar{\mathbf{r}}$ .

## B. Performance Analysis

The MIMO system representation in (10) can be alternatively represented as

$$\mathbf{y}_F = \mathbf{h}_k s(k) + \mathbf{I}_k + \mathbf{z}_F, \quad (28)$$

where  $\mathbf{h}_k$  is the  $k$ -th column of  $\mathbf{G}_F$ , and  $\mathbf{I}_k = \sum_{m \neq k} \mathbf{h}_m s(m)$  represents the ICI related to the symbol  $s(k)$ . The frequency domain noise vector,  $\mathbf{z}_F$ , is a zero mean complex Gaussian random vector with covariance matrix given in (22).

The presence of ICI makes it difficult, if not impossible, to obtain the exact error probability of the OOFDM system in doubly selective fading. Instead, the matched filter bound originally developed for single carrier system [15] is employed here to facilitate the performance analysis by neglecting the ICI component in the equivalent system. The result is a performance lower bound that defines the best performance achievable by the proposed system and quantifies the benefits of Doppler diversity and multipath diversity.

For an OOFDM system operating in a doubly selective Rayleigh fading channel, the frequency domain channel vector,  $\mathbf{h}_k$ , is zero-mean complex Gaussian distributed with covariance matrix  $\mathbf{R}_{h_k} = \mathbb{E}(\mathbf{h}_k \mathbf{h}_k^H)$ . The channel vector  $\mathbf{h}_k$  can be represented as  $\mathbf{h}_k = [\mathbf{h}_k^T(0), \mathbf{h}_k^T(1), \dots, \mathbf{h}_k^T(u-1)]^T$ , where  $\mathbf{h}_k(m) \in \mathcal{C}^{N \times 1}$  is the  $k$ -th column of  $\mathbf{H}_m$ , and the  $(n+1)$ -th element of  $\mathbf{h}_k(m)$  is  $g_{DF}(\frac{n-k}{uN}, \frac{mN+k}{uN})$ . Thus the covariance matrix,  $\mathbf{R}_{h_k}$ , can be written in the form of a block matrix as

$$\mathbf{R}_{h_k} = \begin{bmatrix} \mathbf{R}_{h_k}(0,0) & \mathbf{R}_{h_k}(0,1) & \cdots & \mathbf{R}_{h_k}(0,u-1) \\ \mathbf{R}_{h_k}(1,0) & \mathbf{R}_{h_k}(1,1) & \cdots & \mathbf{R}_{h_k}(1,u-1) \\ \vdots & \ddots & \ddots & \vdots \\ \mathbf{R}_{h_k}(u-1,0) & \mathbf{R}_{h_k}(u-1,1) & \cdots & \mathbf{R}_{h_k}(u-1,u-1) \end{bmatrix}$$

where  $\mathbf{R}_{h_k}(u_1, u_2) = \mathbb{E}[\mathbf{h}_k(u_1) \mathbf{h}_k^H(u_2)]$  is a size- $N$  square matrix with the  $(m+1, n+1)$ -th element being

$$(\mathbf{R}_{h_k}(u_1, u_2))_{m+1, n+1} = \mathbb{E} \left[ g_{DF} \left( \frac{m-k}{uN}, \frac{u_1 N + k}{uN} \right) g_{DF}^* \left( \frac{n-k}{uN}, \frac{u_2 N + k}{uN} \right) \right]. \quad (29)$$

Combining (29) with Lemma 1, we have

$$(\mathbf{R}_{h_k}(u_1, u_2))_{m+1, n+1} = \frac{1}{uN^2} \sum_{v_1, v_2}^{u-1} \sum_{q_1, q_2}^{N-1} \sum_{l_1, l_2}^{L-1} c_{m,n}(uq_1 + v_1, uq_2 + v_2) d_{u_1, u_2}(ul_1 + v_1, ul_2 + v_2), \quad (30)$$

where

$$c_{m,n}(a, b) = J_0(2\pi F_d T_2(a-b)) e^{-j2\pi \frac{(m-k)[a-(n-k)b]}{uN}}, \quad (31)$$

$$d_{u_1, u_2}(a, b) = \rho(a, b) e^{-j2\pi \frac{(u_1 N + k)a - (u_2 N + k)b}{uN}}.$$

With the covariance matrix  $\mathbf{R}_{h_k}$ , the lower bound of the unconditional error probability in doubly selective fading can be obtained by following the similar procedure as described in Section IV-B. The SNR of the interference-free equivalent system is  $\gamma_k = \vartheta_k \gamma_0$ , where  $\vartheta_k = \mathbf{h}_k^H \Phi \mathbf{h}_k$ . The SER lower bound is [15]

$$P(E_k) = \frac{1}{\pi} \int_0^{\frac{\pi}{2}} \prod_{i=1}^{\tilde{v}_k} \left( 1 + \gamma_0 \cdot \frac{\eta_i}{\sin^2 \theta} \right)^{-1} d\theta, \quad (32)$$

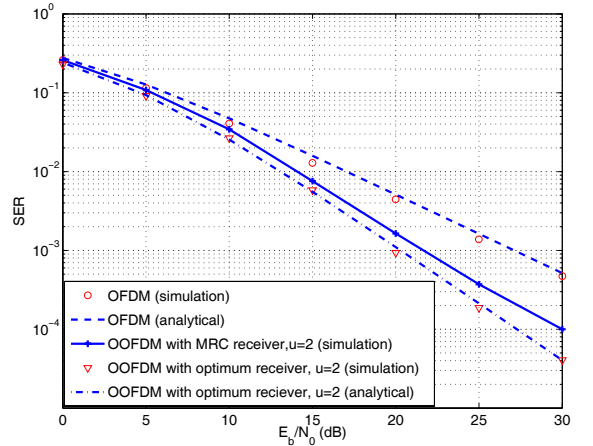


Fig. 2. SER performance of the proposed OOFDM system in a quasi-static fading channel. The number of subcarriers was  $N = 64$  at the transmitter. The oversampling factor of the OOFDM was  $u = 2$ .

where  $\tilde{v}_k$  is the rank of the product matrix  $\mathbf{R}_{h_k} \Phi$ , with  $\eta_i$  being the corresponding eigenvalues. The best performance of the OOFDM system in doubly selective fading depends on the matrices,  $\mathbf{R}_{h_k}$  and  $\Phi$ , which are in turn determined by the maximum Doppler spread,  $F_d$ , the power delay profile,  $G(\tau)$ , and the sampling rate,  $u$ .

## VI. SIMULATION RESULTS

During simulation, the fading channels were generated based on the typical urban (TU) channel power delay profile [23] with the normalized Doppler frequency  $F_d T_0$  being small for quasi-static channels and large for doubly selective channels. The sample period at the transmitter was  $T_1 = 3.69 \mu\text{s}$ . The square root raised cosine (SRRC) filter with roll-off factor,  $\alpha = 1$ , was used as both the transmit and receive filters. The oversampling factor used by the OOFDM system was  $u = 2$  unless specified otherwise.

The performances of the OOFDM and the conventional OFDM systems in quasi-static frequency selective fading were compared. Both systems employed the QPSK modulation with the number of subcarriers at the transmitter being  $N = 64$ . Considerable performance improvement of the OOFDM system over the conventional OFDM system was observed from both simulation and analytical results, as shown in Fig. 2. At the SER level of  $10^{-3}$ , the OOFDM system with optimum receiver outperforms the conventional OFDM system by 7 dB. The performance improvement was mainly contributed by the introduction of multipath diversity. The performance of the OOFDM system with a conventional MRC receiver also outperformed the conventional OFDM thanks to oversampling at the receiver. The MRC receiver directly performed diversity combining over the SIMO system of (15) without considering the correlation among noise samples, and resulted in a performance loss of approximately 2 dB compared to the OOFDM optimum receiver. In all cases of quasi-static fading, good agreement was observed between the simulation results and the theoretical SER expression given in (21).

In Fig. 3 we compared the performance of the proposed OOFDM system with two existing modified OFDM schemes:

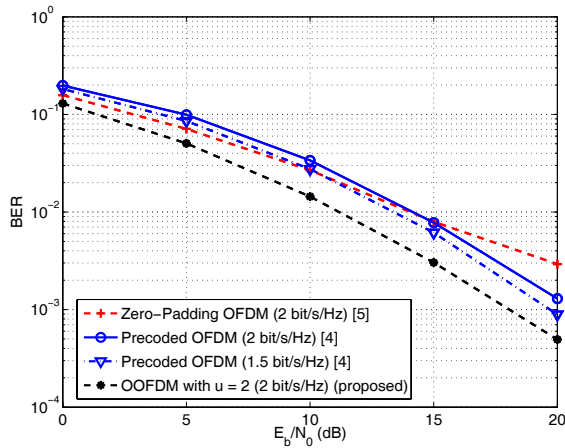


Fig. 3. Comparison of the proposed OOFDM system with existing precoded OFDM and zero-padding OFDM schemes. The number of subcarriers at the transmitter was  $N = 64$  for the OOFDM and ZP-OFDM systems, and  $N = 128$  for the Precoded OFDM with a code rate of  $1/2$ .

the precoded OFDM [2], and the zero-padding OFDM (ZP-OFDM) [3]. The schemes in [2] and [3] achieve multipath diversity in OFDM systems through, respectively, precoding at the transmitter [2], or zero-padding at the receiver [3]. The precoding or zero-padding can lead to an equivalent system that is similar to that achieved through oversampling. The precoded OFDM results in Fig. 3 were obtained with a code rate of  $1/2$ , corresponding to a spectral efficiency of  $2 \text{ bit/s/Hz}$  for a 16QAM modulated system, and  $1.5 \text{ bit/s/Hz}$  for an 8PSK modulated system. QPSK modulation were employed for uncoded OOFDM and ZP-OFDM systems to achieve a spectral efficiency of  $2 \text{ bit/s/Hz}$ . The number of subcarriers at the transmitter was  $64$  for OOFDM and ZP-OFDM, and  $128$  for precoded OFDM to account for the  $1/2$  code rate. The ZP-OFDM is padded to  $256$  subcarriers at the receiver, and both the OOFDM and the precoded OFDM had  $128$  subcarriers at the receiver. Results in Fig. 3 indicated that the proposed OOFDM system consistently outperformed both existing methods with the same or even smaller spectral efficiency. In addition, the existing methods in [2] and [3] can only operate in quasi-static fading, yet the proposed OOFDM scheme can operate in doubly selective fading.

The performances of the OOFDM system and the OFDM system were compared for doubly selective fading in Figs. 4 and 5. The first example used  $N = 16$ . The normalized Doppler spread was  $F_d T_0 = 0.05$ . The DD-BDFE was used in both the OOFDM system and the conventional OFDM system for ICI suppression. The proposed OOFDM system consistently outperformed the conventional OFDM system for both BPSK and 16QAM, as shown in Fig. 4. The analytical lower bound derived for the OOFDM system in doubly selective fading provided a reasonable prediction of the SER with small differences between the lower bound and simulation results. The impact of the normalized Doppler spread  $F_d T_0$  on system performance was evaluated in Fig. 5. At low SNR, both the conventional OFDM system and the OOFDM system benefit from larger values of  $F_d T_0$  due to the larger Doppler diversity. However, at large SNR and high Doppler frequency ( $F_d T_0 = 0.5$ ), an error floor occurred in the conventional

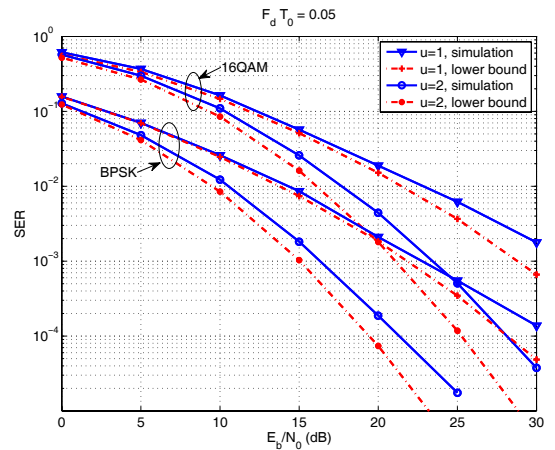


Fig. 4. SER performance of the OOFDM system in a doubly selective fading channel. The normalized Doppler spread was  $F_d T_0 = 0.05$ . The conventional OFDM system is denoted as  $u = 1$ .

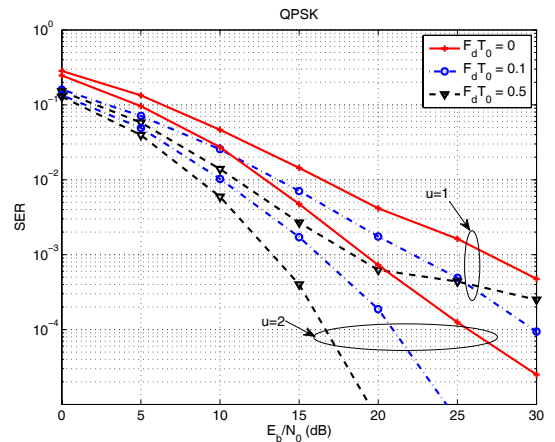


Fig. 5. Impacts of Doppler spread on system performance in quasi-static ( $F_d T_0 = 0$ ) and doubly selective ( $F_d T_0 = 0.1, 0.5$ ) channels. The modulation scheme was QPSK.

OFDM system because the negative effects of ICI dominated over the benefit contributed by Doppler diversity. On the other hand, the OOFDM system was able to harvest the Doppler diversity and suppress the ICI simultaneously leading to consistent performance with the increase of  $F_d T_0$ . At the SER level of  $10^{-3}$ , the OOFDM system outperformed the OFDM by  $7 \text{ dB}$ ,  $6 \text{ dB}$ , and  $5 \text{ dB}$ , for  $F_d T_0 = 0, 0.1$ , and  $0.5$ , respectively.

## VII. CONCLUSIONS

A new oversampled OFDM system operating in doubly selective fading has been presented in this paper. The oversampling at the receiver leads to an equivalent channel model that enables a two dimensional Doppler-frequency grid. The OOFDM system achieves both Doppler diversity and multipath diversity by simultaneously performing coherent combining of data samples and non-coherent combining of ICI over the Doppler-frequency grid, while retaining the same spectral efficiency and similar complexity as the conventional OFDM system. Optimum and sub-optimum receivers have been developed and their respective theoretical error probabilities have

been derived. Both theoretical analysis and computer simulations showed that considerable performance improvements of as much as 7 dB can be achieved by the OOFDM system over the conventional OFDM or other existing modified OFDM systems under a wide range of system configurations. More interestingly, simulation study showed that the conventional OFDM system exhibits an error floor at high Doppler spread in the high SNR region due to the dominance of ICI, while the proposed OOFDM system can improve the SER performance consistently with the increase of the Doppler spread thanks to its inherent ICI suppression ability. An oversampling factor of two is sufficient to collect most of the benefits of the OOFDM system while keeping the complexity similar to the conventional OFDM system.

## REFERENCES

- [1] R. V. Nee and R. Prasad, *OFDM for Wireless Multimedia Communications*. Artech House Publisher, 2000.
- [2] X.-G. Xia, "Precoded and vector OFDM robust to channel spectral nulls and with reduced cyclic prefix length in single transmit antenna systems," *IEEE Trans. Commun.*, vol. 49, pp. 1363-1374, Aug. 2001.
- [3] J. Wang, J. Song, Z.-X. Yang, and J. Wang, "Frames theoretic analysis of zero-padding OFDM over deep fading wireless channels," *IEEE Trans. Broadcast.*, vol. 52, pp. 252-260, June 2006.
- [4] Z. Liu, Y. Xin, and G. B. Giannakis, "Linear constellation precoding for OFDM with maximum multipath diversity and coding gains," *IEEE Trans. Commun.*, vol. 51, pp. 416-427, Mar. 2003.
- [5] H.-C. Wu, "Analysis and characterization of intercarrier and interblock interferences for wireless mobile OFDM systems," *IEEE Trans. Broadcast.*, vol. 52, pp. 203-210, June 2006.
- [6] S. Chen and C. Zhu, "ICI and ISI analysis and mitigation for OFDM systems with insufficient cyclic prefix in time varying channels," *IEEE Trans. Consumer Electron.*, vol. 50, pp. 78-83, Feb. 2004.
- [7] S. Chen and T. Yao, "Low complexity ICI cancellation for OFDM systems in doubly selective fading channels," in *Proc. IEEE Int'l. Conf. Commun. ICC'04*, June 2004, vol. 5, pp. 2535-2538.
- [8] T. Wang, J. G. Proakis, and J. R. Zeidler, "Techniques for suppression of intercarrier interference in OFDM systems," in *Proc. IEEE Wireless Commun. Netw. Conf. WCNC'05*, vol. 1, pp. 39-44, Mar. 2005.
- [9] L. Tadjpour, S.-H. Tsai, and C.-C. J. Kuo, "An approximately MAI-free multiaccess OFDM system in fast time varying channels," *IEEE Trans. Signal Process.*, vol. 55, pp. 3787-3799, July 2007.
- [10] Y.-P. Lin and S.-M. Phoong, "Window designs for DFT-based multi-carrier systems," *IEEE Trans. Signal Process.*, vol. 53, pp. 1015-1024, Mar. 2005.
- [11] X. Ma and G. B. Giannakis, "Maximum-diversity transmissions over time-selective wireless channels," in *Proc. IEEE Wireless Commun. Netw. Conf. WCNC'02*, vol. 1, pp. 497-501, Mar. 2002.
- [12] J. Wu, "Exploring maximum Doppler diversity by Doppler domain multiplexing," in *Proc. IEEE Global Telecommun. Conf. GLOBECOM'06*, Nov. 2006, pp. 1-5.
- [13] G. Ungerboeck, "Fractional tap-spacing equalizer and consequences for clock recovery in data modems," *IEEE Trans. Commun.*, vol. COM-24, pp. 856-864, Aug. 1976.
- [14] K. J. Molnar, G. E. Bottomley, and R. Ramesh, "A novel fractionally-spaced MLSE receiver and channel tracking with side information," in *Proc. IEEE Veh. Technol. Conf. VTC'98 Spring*, vol. 3, pp. 2251-2255, May 1998.
- [15] J. Wu, Y. R. Zheng, K. B. Letaief, and C. Xiao, "On the error performance of wireless systems with frequency selective fading and receiver timing phase offset," *IEEE Trans. Wireless Commun.*, vol. 6, pp. 720-729, Feb. 2007.
- [16] M. Sharif, M. Gharavi-Alkhansari, and B. H. Khalaj, "On the peak-to-average power of OFDM signals based on oversampling," *IEEE Trans. Commun.*, vol. 51, pp. 72-78, Jan. 2003.
- [17] S. Roy and C. Li, "A subspace blind channel estimation method for OFDM systems without cyclic prefix," *IEEE Trans. Wireless Commun.*, vol. 1, pp. 572-579, Oct. 2002.
- [18] B. Chen and H. Wang, "Blind estimation of OFDM carrier frequency offset via oversampling," *IEEE Trans. Signal Process.*, vol. 52, pp. 2047-2057, July 2004.
- [19] C. Tepedelenlioglu and R. Challagulla, "Low-complexity multipath diversity through fractional sampling in OFDM," *IEEE Trans. Signal Process.*, vol. 52, pp. 3104-3116, Nov. 2004.
- [20] Y.-S. Lee and B.-S. Seo, "OFDM receivers using oversampling with rational sampling ratios," *IEEE Trans. Consumer Electron.*, vol. 55, pp. 1765-1770, Nov. 2009.
- [21] C. Xiao, J. Wu, S.-Y. Leong, Y. R. Zheng, and K. B. Letaief, "A discrete-time model for spatio-temporally correlated MIMO WSSUS multipath Channels," *IEEE Trans. Wireless Commun.*, vol. 3, pp. 1678-1688, Sep. 2004.
- [22] J. Wu and Y. R. Zheng, "Low complexity soft-input soft-output block decision feedback equalization," *IEEE J. Sel. Areas Commun.*, vol. 26, pp. 281-289, Feb. 2008.
- [23] ETSI. GSM 05.05, "Radio transmission and reception," ETSI EN 300 910 V8.5.1, Nov. 2000.



**Jingxian Wu** (S'02-M'06) received the B.S. degree in electronic engineering from Beijing University of Aeronautics and Astronautics, Beijing, China, in 1998, the M.S. degree in electronic engineering from Tsinghua University, Beijing, China, in 2001, and the Ph.D. degree in electrical engineering from the University of Missouri, Columbia, in 2005. He is currently an Assistant Professor with the Department of Electrical Engineering, University of Arkansas, Fayetteville. His research interests mainly focus on wireless communications and wireless networks,

including ultra-low power communications, cooperative communications, compressive sensing, and cross-layer optimization, etc. He is currently an Associate Editor of the IEEE TRANSACTIONS ON VEHICULAR TECHNOLOGY. He served as a Student Program Cochair of the 2010 Global Telecommunication Conference, a Cochair for the 2009 Wireless Communication Symposium of the IEEE Global Telecommunications Conference, and a Student Travel Grant Chair for the 2010 IEEE International Conference on Communications. Since 2006, he has served as a Technical Program Committee Member for a number of international conferences, including the IEEE Global Telecommunications Conference, the IEEE Wireless Communications and Networking Conference, and the IEEE International Conference on Communications.



**Yahong Rosa Zheng** received the B.S. degree from the University of Electronic Science and Technology of China, Chengdu, China, in 1987, and the M.S. degree from Tsinghua University, Beijing, China, in 1989, both in electrical engineering. She received the Ph.D. degree from the Department of Systems and Computer Engineering, Carleton University, Ottawa, Canada, in 2002. She was an NSERC Postdoctoral Fellow from Jan. 2003 to April 2005 at the University of Missouri-Columbia. Currently, she is an assistant professor with the Department of Electrical

and Computer Engineering at the Missouri University of Science and Technology (formerly the University of Missouri-Rolla). Her research interests include array signal processing, space-time adaptive processing, wireless communications, and wireless sensor networks. She has served as an associate editor for IEEE TRANSACTIONS ON WIRELESS COMMUNICATIONS 2006-2008 and as a Technical Program Committee (TPC) member for many IEEE international conferences, including IEEE Vehicular Technol. Conf., IEEE GlobeCom, and IEEE Intl. Conf. Commun., etc. She is the recipient of an NSF CAREER award in 2009.